Chinese Chemical Letters 36 (2025) 109818

Contents lists available at ScienceDirect

Chinese Chemical Letters

journal homepage: www.elsevier.com/locate/cclet

Desymmetrized pillar[8]arenes: High-yield synthesis, functionalization, and host-guest chemistry

Jie Yang[a,b], Xin-Yue Lou[a], Dihua Dai[a], Jingwei Shi[c,*], Ying-Wei Yang[a,*]

[a] College of Chemistry, Jilin University, Changchun 130012, China
[b] School of Life Sciences, Jilin University, Changchun 130012, China
[c] Department of Laboratory Medicine Center, China-Japan Union Hospital of Jilin University, Changchun 130033, China

ARTICLE INFO

Article history:
Received 30 January 2024
Revised 12 March 2024
Accepted 22 March 2024
Available online 24 March 2024

Keywords:
Host-guest interaction
Macrocycle chemistry
Pillararenes
Supramolecular chemistry
Synthetic macrocycles

ABSTRACT

The preparation, functionalization, and investigations in host-guest properties of high-level pillararene macrocycles have long been a big challenge because of the lack of efficient synthetic methods. Herein, a novel type of pillararene derivative, namely desymmetrized pillar[8]arene (DP[8]A), has been successfully synthesized *via* a facile two-step strategy with high yield. Compared with its pillar[8]arene counterpart, DP[8]A is composed of four alkoxy-substituted benzene units and four bare benzene rings. Single crystal analysis has been performed in order to unveil the molecular conformation and packing mode of DP[8]A, which indicated that DP[8]A possesses a unique chair-like structure and much smaller steric hindrance. Density functional theory (DFT) calculations and electrostatic potential map suggested the inhomogeneous electronic distribution in the DP[8]A cavity. Water-soluble carboxylate-modified DP[8]A, that is, CDP[8]A, was also prepared to investigate the host-guest properties in aqueous solution with methyl viologen (MV), where the binding constant and morphologies of the formed host-guest complexes have been studied. In all, this new version of eight-membered pillararene derivative might potentially serve as a powerful macrocycle candidate for further applications in supramolecular chemistry.

The design and synthesis of new macrocycles with well-defined conformations and distinct properties has been one of the cutting-edge topics in supramolecular chemistry. Macrocyclic hosts with more aromatic moieties and larger cavity sizes have attracted tremendous attention due to their appealing topological architectures and selective molecular recognition properties. More recently, several newly designed large-scale supramolecular macrocycles, including quaterphen[*n*]arenes [1], Ex^{n}Box cyclophanes [2], elongated geminiarene [3], pagoda[5]arene [4], and many others [5–7] with particular recognition abilities have been widely investigated.

Pillar[*n*]arenes, first synthesized by Ogoshi and co-workers in 2008, have attracted much attention in recent years owing to their stable and symmetric columnar conformations, facile modification, unique host-guest properties, and relatively high yields [8–18]. Notably, the high-level pillar[*n*]arenes ($n \geq 7$, HLPAs) are important parts of pillararenes, and their investigation is closely related to the evolvement of pillararenes and supramolecular macrocyclic fields. However, the research progress of HLPAs lags far behind pillar[5,6]arenes because of the lack of proper synthetic methods, low synthetic yields, and difficulties in post-synthetic modification. Compared with the significant advances and extensive applications in pillar[5,6]arenes, there were only a few reports on the HLPAs and their functionalized derivatives [19–22]. Therefore, it is highly urgent to explore the preparation of new HLPAs to enrich the pillararene's toolbox and expand the application prospects of their research systems. In addition, the nanosized cavities, low steric hindrance, and flexible skeletons of HLPAs endow them with the capability of structural changes and conformational adaptability induced by guests [23]. Nonetheless, although increasing the number of monomers and building blocks can facilely obtain high-level macrocyclic hosts, the steric hindrance would also be dramatically increased at the same time. For instance, most of the representative high-level supramolecular macrocycles such as calix[8–10]arenes [24–27], cucurbit[13–15]urils [28–30], pillar[8–10]arenes [10,31-35], and asar[8–11]arenes [36] exhibit complex conformations, which strongly indicate that the preparation of large-sized macrocycles with low steric hindrance remains a significant challenge.

Inspired by the synthetic methodology of cyclophanes and pillararenes, our group developed a two-step strategy for the preparation of [2]biphenyl-extended pillar[6]arene [37–40], which is

* Corresponding authors.
E-mail addresses: shijingwei@jlu.edu.cn (J. Shi), ywyang@jlu.edu.cn (Y.-W. Yang).

https://doi.org/10.1016/j.cclet.2024.109818
1001-8417/

considered as an elongated version of pillar[6]arene homolog, which pre-connected 1,4-dimethoxybenzene with diphenyl blocks through Friedel-Crafts alkylation reaction to obtain an intermediate molecule (MDM) and then reacted the MDM with paraformaldehyde under the catalysis of $BF_3{\cdot}OEt_2$. Subsequently, we synthesized leaning tower[6]arenes *via* the two-step strategy [41–44], which possessed enhanced cavity adaptability, decreased steric hindrance, and improved synthetic versatility compared with the traditional pillar[6]arene. Impressed by the procedure of structuring extended and desymmetrized macrocyclic arenes, we envision that taking advantage of the two-step strategy will hopefully lead to selectively defunctionalized HLPAs with fascinating structural features and higher yields, further promoting the evolution of pillararene family. Particularly, gram-scale synthesis of pillar[8]arene is hard to accomplish due to the harsh reaction conditions, low yields, multiple by-products, and complicated post-treatment procedures [45]. Since the pillar[8]arene was synthesized with a low yield of 1%, there has been no further research on its functionalization and applications over the past decade. Notably, to the best of our knowledge, no examples of functionalized pillar[8]arenes have been reported yet. Herein, directed by the two-step strategy, we present the synthesis of a newly designed desymmetrized pillar[8]arene analog, which bears four dealkoxylated benzene-bridged units, namely desymmetrized pillar[8]arene (DP[8]A). The synthetic yield of DP[8]A can reach 37%, providing opportunities for further functionalization.

The synthetic route to DP[8]A *via* the facile two-step strategy was successfully implemented, as shown in Fig. 1. First, compound **1** was substituted with 1,4-dimethoxybenzene in the presence of $AlCl_3$ through a Friedel–Crafts alkylation reaction, giving a synthetic intermediate, namely MDM-DP[8]A (40.2% yield, Fig. S1 in Supporting information). The obtained MDM-DP[8]A was then reacted with paraformaldehyde in various solvents with different catalysts (Tables S1 and S2 in Supporting information) to select the most appropriate conditions, whereby the catalysis of CF_3COOH in 1,2-dichloroethane was proved to be most efficient in the synthesis of DP[8]A (37% yield, Figs. S2-S4 in Supporting information). Compared with the traditional method that can only obtain a trace amount of pillar[8]arene as the by-product of pillar[5,6]arene, this two-step strategy demonstrates a dramatic leap in terms of synthetic methodology, which provides a proficient approach for gram-scale preparation of eight-membered pillararene analogs, thus allowing for in-depth studies on DP[8]A derivatives and their potential applications.

The single crystals of DP[8]A were grown *via* a solvent diffusion method in the mixed solvent of dichloromethane and hexane, and the single crystal data was shown in Table S1. Compared with the well-defined pillar-shaped P[8]A, DP[8]A possesses a twisted macrocyclic structure attributing to the absence of alkoxy groups on the four benzenes located on the two extended sides of the macrocycle (Figs. 2a and b). According to the single crystal analysis results, the dihedral angle between the unsubstituted benzene rings is 51.72°, while the angle between the methoxy–substituted benzene rings is 65.25° (Figs. S5 and S6 in Supporting information). Besides, the angle between the unsubstituted rings and their adjacent methylene carbon atom-based plane is 72.66°, and the angle

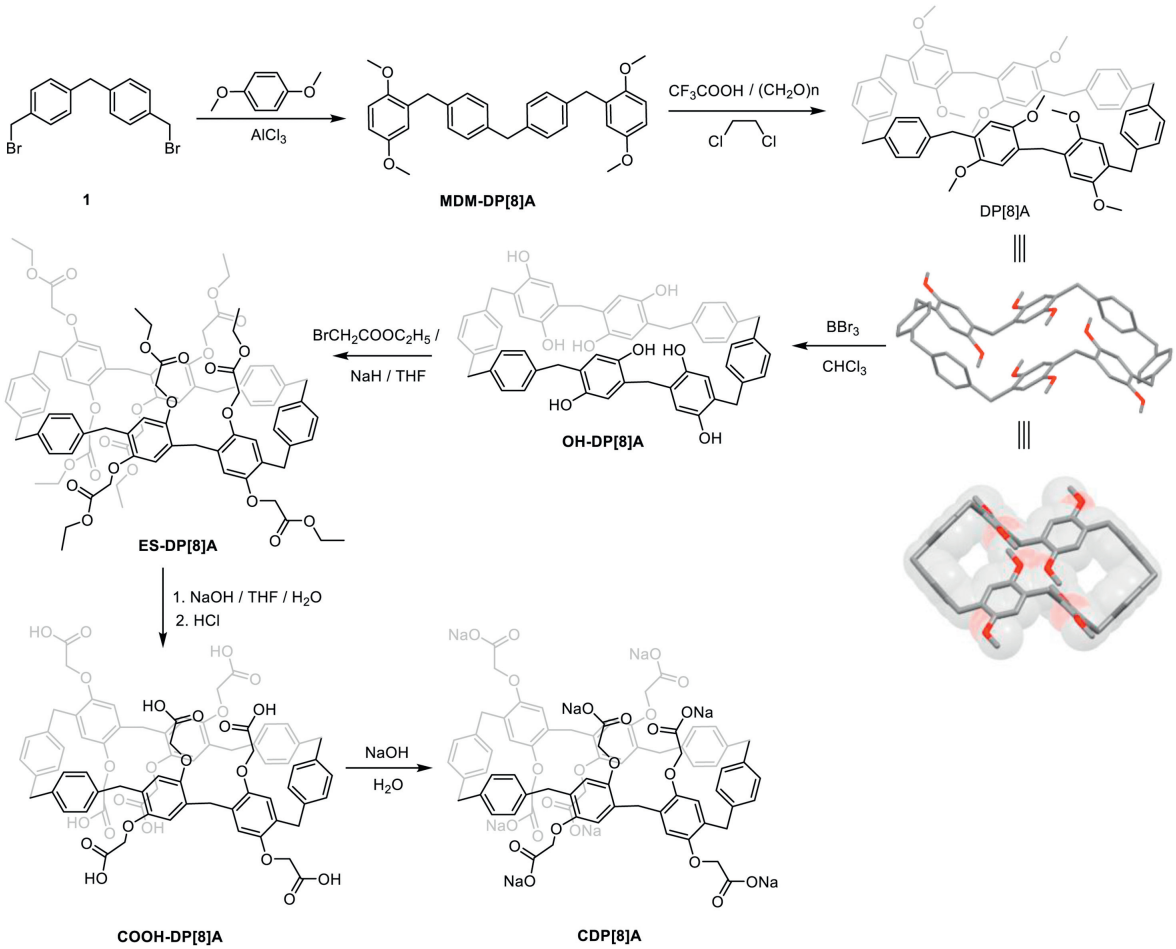

Fig. 1. The synthetic route to DP[8]A and its functionalization.

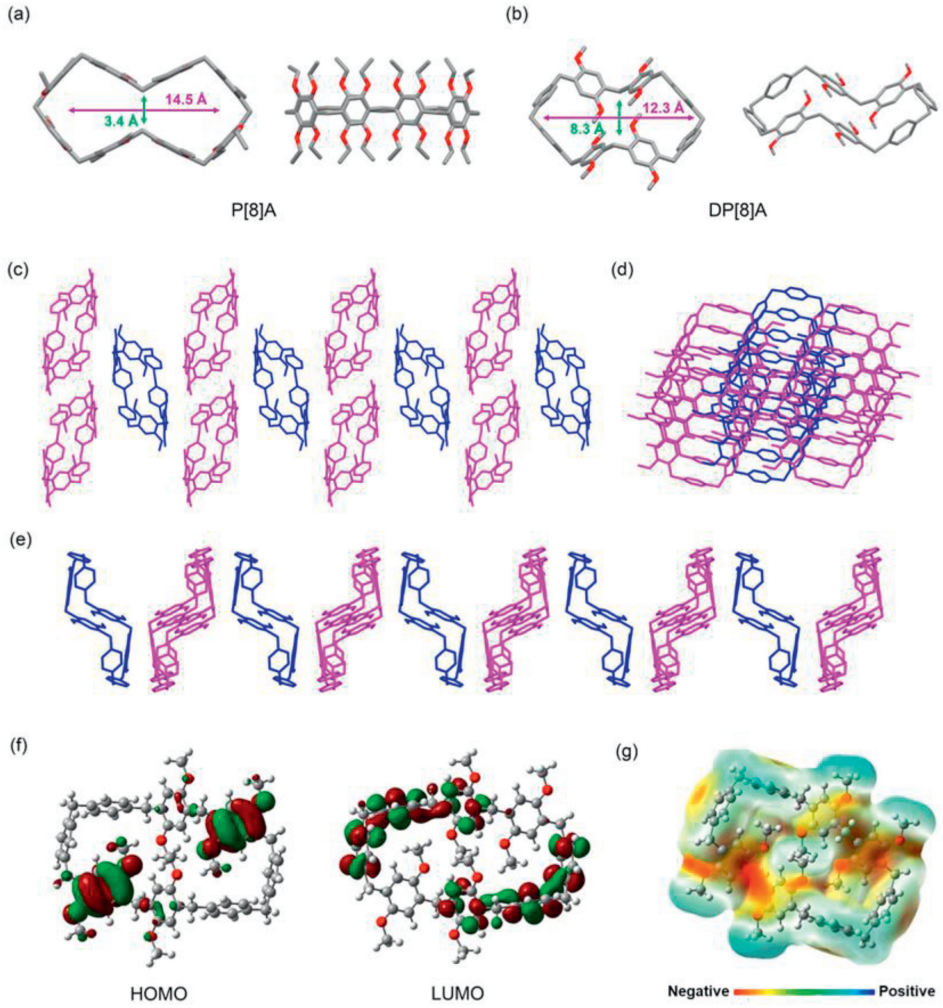

Fig. 2. Crystal structures and cavity sizes of (a) P[8]A and (b) DP[8]A (top view and side view). Packing mode of DP[8]A viewed along the (c) [100], (d) [010], and (e) [001] directions. Hydrogen atoms were omitted for clarity. Oxygen atoms are shown in red and carbon atoms are shown in grey. (f) HOMO and LUMO orbitals of DP[8]A. (g) Electrostatic potential map of DP[8]A.

between the unsubstituted ring and the methoxy substituted ring-based plane is 7.51° (Fig. S7 in Supporting information). Hence, with the opposite benzenes parallel to each other and the neighboring phenyl units arranged in a tilted manner, DP[8]A is endowed with a chair conformation instead of the rigid columnar architecture. In addition, the packing mode of DP[8]A in the single crystal was also investigated. An AB-typed layer-by-layer stacking structure can be spotted from the (1,0,0) direction, whereby the DP[8]A molecules in two adjoining layers are arranged in the opposite direction (Fig. 2c). As a result, the elongation of this packing mode leads to the formation of 1D cavity channels that overlap with each other (Fig. 2d). Interestingly, along the (0,0,1) direction, the opposite arrangement of adjacent layers can be observed more clearly, showing a resemblance of rows of chairs (Fig. 2e). This unique stacking pattern has been highly stabilized due to the multiple C–H···O interactions and π-π interactions that exist among the layers (Fig. S8 in Supporting information). Besides single crystal analysis, density functional theory (DFT) calculations were also performed to better understand the electronic properties of DP[8]A cavity. As shown in Fig. 2f, the highest occupied molecular orbital (HOMO) and lowest unoccupied molecular orbital (LUMO) are separated, indicating the inhomogeneous electronic distribution within the cavity, where HOMO occupies the methoxy–substituted region, while LUMO is mainly located at the unsubstituted benzene rings. Similar evidence was provided by the electrostatic potential map of DP[8]A, signifying the higher electron density of substituted phenyl groups compared with the bare benzenes (Fig. 2g).

Subsequently, in order to further functionalize this new type of macrocycle, water-soluble carboxylate-functionalized DP[8]A (CDP[8]A) was successfully prepared with high yield (Fig. 1). To realize the perfunctionalization of the substituent group in DP[8]A, we first conducted a demethylation reaction of DP[8]A with an excessive amount of BBr_3 to afford the hydroxy version of DP[8]A (OH-DP[8]A, Figs. S9-S11 in Supporting information). Subsequently, ES-DP[8]A was obtained with a satisfactory yield through nucleophilic substitution on OH-DP[8]A with excess ethyl bromoacetate (Figs. S12-S14 in Supporting information), and the hydrolysis of ES-DP[8]A was performed under basic conditions followed by the treatment of HCl, generating carboxylic acid-substituted DP[8]A (COOH-DP[8]A) with a high yield of 90% (Figs. S5-S17 in Supporting information). Finally, CDP[8]A was facilely obtained by treating COOH-DP[8]A with sodium hydroxide (Figs. S18-S20 in Supporting information).

Inspired by the efficient capture or antagonism of highly toxic molecules by supramolecular macrocycles [46,47], the host-guest binding mode between CDP[8]A and the positively charged guest molecule, methyl viologen (MV, one of the most widely used herbicides in the world), was investigated in aqueous solutions. According to the ^{1}H NMR spectra, the signals of protons (H_1, H_2, and

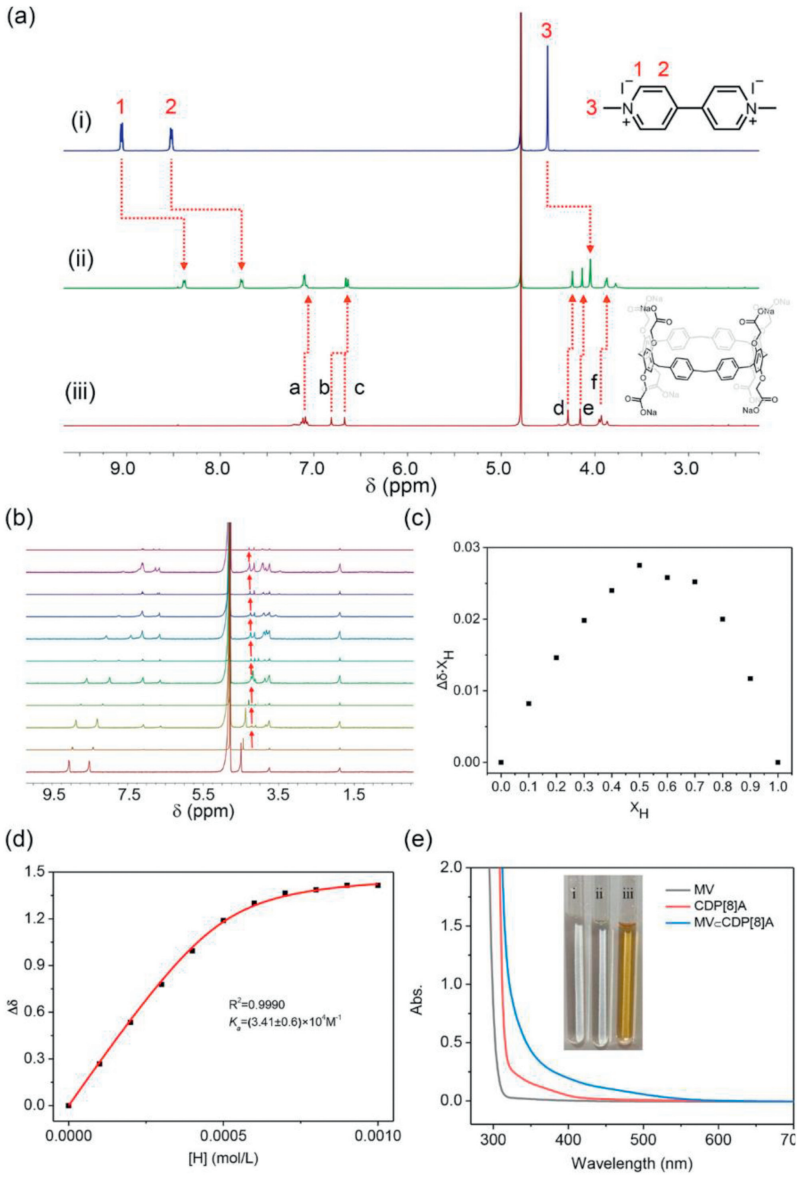

Fig. 3. (a) Partial ^{1}H NMR spectra (400 MHz, D_2O, 298 K) of (i) MV (5 mmol/L), (ii) CDP[8]A and MV (5 mmol/L each), and (iii) CDP[8]A (5 mmol/L). (b) ^{1}H NMR spectra of different ratios of CDP[8]A and MV (from top to bottom: CDP[8]A: MV = 10:0, 9:1, 8:2, 7:3, 6:4, 5:5; 4:6, 3:7, 2:8, 1:9 and 0:10). (c) Job's plot analysis of CDP[8]A and MV. (d) Changes in the chemical shift of MV (0.5 mmol/L) upon gradual addition of CDP[8]A (0–1 mmol/L) and the non-linear fitting curve of the plot. (e) UV–vis spectra of MV (1 mmol/L), CDP[8]A (1 mmol/L), and MV⊂CDP[8]A (1 mmol/L). Inset: photographs of (i) MV (5 mmol/L), (ii) CDP[8]A (5 mmol/L), and (iii) MV⊂CDP[8]A (5 mmol/L).

H_3) on MV undergo observable upfield shifts ($\Delta\delta = -0.67$, -0.751, and -0.457 ppm, respectively) upon the addition of CDP[8]A in D_2O, which suggests the shielding effect caused by the encapsulation of MV into CDP[8]A cavity (Fig. 3a). Changes in the chemical shifts can also be spotted for the protons of CDP[8]A. In addition, 2D DOSY NMR spectra of MV alone and MV⊂CDP[8]A were also collected (Fig. S21 in Supporting information), indicating that the diffusion coefficient (D) of the mixture (3.16×10^{-10} m^2/s) was lower than that of MV (5.69×10^{-10} m^2/s). To determine the stoichiometry and binding constant (K_a) between CDP[8]A and MV, NMR titration experiments were carried out. The binding stoichiometry was 1:1 according to the Job's plot method (Figs. 3b and c), and the K_a value was calculated to be $(3.41 \pm 0.6) \times 10^4$ L/mol by the non-linear curve-fitting method (Fig. 3d and Fig. S22 in the Supporting information), which was carefully compared with other reported water-soluble pillararene derivatives for better understanding (Table S4 in the Supporting information). Interestingly, as MV was encapsulated by CDP[8]A, its transparent colorless solution immediately turned yellow. According to the UV–vis absorption spectra, this color change can be ascribed to the charge transfer behavior between CDP[8]A cavity and electron-deficient MV (Fig. 3e), demonstrating that the electronic interaction has significantly contributed to the host-guest complexation.

Moreover, the assembly morphology of MV⊂CDP[8]A in aqueous solution was also investigated. Scanning electron microscopy (SEM) images of MV, CDP[8]A, and MV⊂CDP[8]A were collected. Distinct from the bulky CDP[8]A aggregates and amorphous MV assemblies (Figs. 4a and b), MV⊂CDP[8]A adopted a well-defined bundle-shaped structure (Figs. 4c and d), which suggests that the formation of host-guest complexes has led to the ordered assembly in a linear pattern. This exciting phenomenon demonstrates the possibilities of CDP[8]A in forming propagated, well-ordered structures with the assistance of host-guest and electrostatic interactions, indicating application potentials in functional supramolecular assemblies for mimicking biological macromolecules.

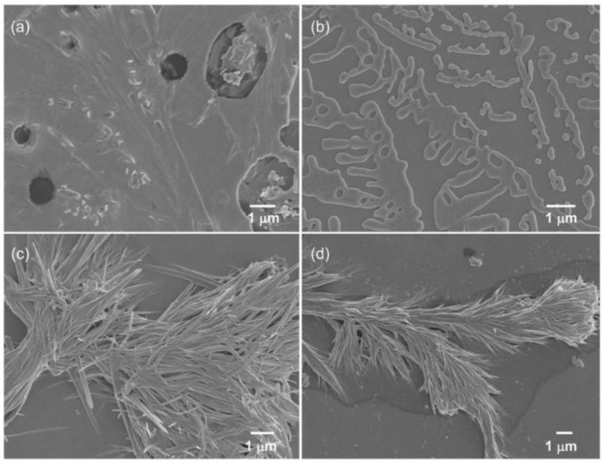

Fig. 4. SEM images of (a) CDP[8]A (5 mmol/L), (b) MV (5 mmol/L), and (c, d) MV⊂CDP[8]A (5 mmol/L each) in aqueous solution.

In conclusion, a novel type of high-level pillararenes denoted as DP[8]A has been designed and synthesized with high yield *via* a convenient two-step strategy. Its unique chair-like conformation, layer-by-layer stacking mode, and inner-cavity electron distribution were investigated by single-crystal analysis and DFT calculations. The water-soluble version of DP[8]A, namely CDP[8]A, was obtained by percarboxylation, and the host-guest interactions between CDP[8]A and MV have been studied in aqueous media, of which a 1:1 binding stoichiometry was confirmed by NMR measurements. Notably, the supramolecular assembly formed by the host-guest complexes adopted a well-defined bundle-shaped morphology, suggesting a regulated aggregating pattern. We believe that the creation of DP[8]A would contribute to expanding the pillararene family and spur the development of novel high-level supramolecular macrocycles. In addition, we envision that the new macrocycle can be applied in the fabrication of various supramolecular materials after further functionalization on its rims, such as supramolecular polymers, drug-loading vesicles, and even organic-inorganic hybrid nanocomposites by integrating with metallic nanomaterials, taking advantage of its high yield, convenient modification, and host-guest properties.

Declaration of competing interest

The authors declare that they have no known competing financial interests or personal relationships that could have appeared to influence the work reported in this paper.

The author is an Editorial Board Member/Editor-in-Chief/Associate Editor/Guest Editor for *Chinese Chemical Letters* and was not involved in the editorial review or the decision to publish this article.

Acknowledgments

We thank the Natural Science Foundation of Jilin Province (No. 20230101052JC), the National Natural Science Foundation of China (Nos. 52173200 and 52203138), and the Jilin Province Science and Technology Development Plan Project (No. #YDZJ202201ZYTS523) for financial support.

Supplementary materials

Supplementary material associated with this article can be found, in the online version, at doi:10.1016/j.cclet.2024.109818.

References

[1] J. Chen, Q. Meng, Y. Zhang, et al., Angew. Chem. Int. Ed. 60 (2021) 11288–11293.
[2] J.C. Barnes, M. Juríček, N.L. Strutt, et al., J. Am. Chem. Soc. 135 (2012) 183–192.
[3] J.R. Wu, Y. Wang, Y.W. Yang, Small 16 (2020) 2003490.
[4] X.N. Han, Q.S. Zong, Y. Han, C.F. Chen, CCS Chem. 4 (2022) 318–330.
[5] M. Dong, X. Liu, Z.Y. Zhang, et al., Chem. Commun. 58 (2022) 2319–2322.
[6] J.C. Barnes, M. Juríček, N.A. Vermeulen, E.J. Dale, J.F. Stoddart, J. Org. Chem. 78 (2013) 11962–11969.
[7] R. Gupta, G. Kumar, R. Gupta, Inorg. Chem. 61 (2022) 7682–7699.
[8] T. Ogoshi, S. Kanai, S. Fujinami, T.A. Yamagishi, Y. Nakamoto, J. Am. Chem. Soc. 130 (2008) 5022–5023.
[9] X.Y. Lou, Y.W. Yang, Adv. Mater. 32 (2020) 2003263.
[10] X.B. Hu, Z. Chen, L. Chen, et al., Chem. Commun. 48 (2012) 10999–11001.
[11] N.L. Strutt, H. Zhang, S.T. Schneebeli, J.F. Stoddart, Acc. Chem. Res. 47 (2014) 2631–2642.
[12] G. Yu, X. Chen, Theranostics 9 (2019) 3041–3074.
[13] K. Wang, J.H. Jordan, K. Velmurugan, et al., Angew. Chem. Int. Ed. 60 (2021) 9205–9214.
[14] X. Zhang, Q. Cheng, L. Li, et al., Theranostics 9 (2019) 3107–3121.
[15] W. Feng, M. Jin, K. Yang, Y. Pei, Z. Pei, Chem. Commun. 54 (2018) 13626–13640.
[16] H. Zhang, Z. Liu, Y. Zhao, Chem. Soc. Rev. 47 (2018) 5491–5528.
[17] S. Cao, L. Song, H. Zhang, J. Han, Y. Zhao, Chin. Chem. Lett. 34 (2023) 108479.
[18] W. Yang, W. Zhang, J. Chen, J. Zhou, Chin. Chem. Lett. 35 (2024) 108740.
[19] Y. Chen, H.Q. Tao, Y.H. Kou, et al., Chin. Chem. Lett. 23 (2012) 509–511.
[20] J. Yang, X. Chi, Z. Li, et al., Org. Chem. Front. 1 (2014) 630–633.
[21] X. Chi, X. Ji, D. Xia, F. Huang, J. Am. Chem. Soc. 137 (2015) 1440–1443.
[22] X. Chi, G. Yu, L. Shao, J. Chen, F. Huang, J. Am. Chem. Soc. 138 (2016) 3168–3174.
[23] J.R. Wu, G. Wu, Y.W. Yang, Acc. Chem. Res. 55 (2022) 3191–3204.
[24] S.H. Dale, M.R.J. Elsegood, C. Redshaw, CrystEngComm 5 (2003) 368–373.
[25] M. Ferchichi, E. Jeanneau, B. Fenet, et al., Tetrahedron Lett. 53 (2012) 4047–4050.
[26] S. Bouoit-Montésinos, F. Vocanson, J. Bassus, R. Lamartine, Synth. Commun. 30 (2000) 911–915.
[27] M. Perrin, N. Ehlinger, L. Viola-Motta, et al., J. Inclusion Phenom. Macrocyclic Chem. 39 (2001) 273–276.
[28] Q. Li, S.C. Qiu, J. Zhang, et al., Org. Lett. 18 (2016) 4020–4023.
[29] X.J. Cheng, L.L. Liang, K. Chen, et al., Angew. Chem. Int. Ed. 52 (2013) 7252–7255.
[30] Q. Li, J. Sun, J. Zhou, et al., Org. Chem. Front. 5 (2018) 1940–1944.
[31] H. Kono, Y. Li, R. Zanasi, et al., J. Am. Chem. Soc. 145 (2023) 8939–8946.
[32] Z. Li, J. Yang, G. Yu, et al., Chem. Commun. 50 (2014) 2841–2843.
[33] G. Yu, J. Zhou, X. Chi, Macromol. Rapid Commun. 36 (2015) 23–30.
[34] Y. Ding, W. Yu, R. Shen, et al., Adv. Healthcare Mater. 12 (2023) 2303308.
[35] Y. Ding, Y. Ma, L. Zhu, et al., J. Mater. Chem. B 10 (2022) 6181–6186.
[36] S.T. Schneebeli, C. Cheng, K.J. Hartlieb, et al., Chem. Eur. J. 19 (2013) 3860–3868.
[37] B. Gao, L.L. Tan, N. Song, K. Li, Y.W. Yang, Chem. Commun. 52 (2016) 5804–5807.
[38] D. Dai, Z. Li, J. Yang, et al., J. Am. Chem. Soc. 141 (2019) 4756–4763.
[39] D. Dai, J. Yang, Y.C. Zou, et al., Angew. Chem. Int. Ed. 60 (2021) 8967–8975.
[40] J.R. Wu, C.Y. Wang, Y.C. Tao, et al., Eur. J. Org. Chem. 2018 (2018) 1321–1325.
[41] J.R. Wu, A.U. Mu, B. Li, et al., Angew. Chem. Int. Ed. 57 (2018) 9853–9858.
[42] Z. Liu, J. Wu, C. Wang, et al., Chin. Chem. Lett. 30 (2019) 2299–2303.
[43] X. Wang, J.R. Wu, F. Liang, Y.W. Yang, Org. Lett. 21 (2019) 5215–5218.
[44] Y. Zhang, Z. Li, S. Meng, A. Dong, Y.W. Yang, Chem. Commun. 58 (2022) 649–652.
[45] T. Ogoshi, N. Ueshima, F. Sakakibara, T.A. Yamagishi, T. Haino, Org. Lett. 16 (2014) 2896–2899.
[46] J. Yang, D. Dai, L. Ma, Y.W. Yang, Chin. Chem. Lett. 32 (2021) 729–734.
[47] S.B. Yu, W. Zhou, J. Tian, et al., Sci. Sin. Chim. 53 (2023) 2345–2356.